Article

A Hybridization of Dragonfly Algorithm Optimization and Angle Modulation Mechanism for 0-1 Knapsack Problems

Lin Wang , Ronghua Shi and Jian Dong *

School of Computer Science and Engineering Central South University, Changsha 410083, China; csuwanglin@csu.edu.cn (L.W.); shirh@csu.edu.cn (R.S.)
* Correspondence: dongjian@csu.edu.cn

Abstract: The dragonfly algorithm (DA) is a new intelligent algorithm based on the theory of dragonfly foraging and evading predators. DA exhibits excellent performance in solving multimodal continuous functions and engineering problems. To make this algorithm work in the binary space, this paper introduces an angle modulation mechanism on DA (called AMDA) to generate bit strings, that is, to give alternative solutions to binary problems, and uses DA to optimize the coefficients of the trigonometric function. Further, to improve the algorithm stability and convergence speed, an improved AMDA, called IAMDA, is proposed by adding one more coefficient to adjust the vertical displacement of the cosine part of the original generating function. To test the performance of IAMDA and AMDA, 12 zero-one knapsack problems are considered along with 13 classic benchmark functions. Experimental results prove that IAMDA has a superior convergence speed and solution quality as compared to other algorithms.

Keywords: angle modulation mechanism; trigonometric generating function; dragonfly algorithm; binary optimization; 0-1 knapsack problem

check for updates

Citation: Wang, L.; Shi, R.; Dong, J. A Hybridization of Dragonfly Algorithm Optimization and Angle Modulation Mechanism for 0-1 Knapsack Problems. *Entropy* **2021**, *23*, 598. https://doi.org/10.3390/e23050598

Academic Editor: Giulia De Masi

Received: 27 February 2021
Accepted: 10 May 2021
Published: 12 May 2021

1. Introduction

Being some of the most important and widely used algorithms, gradient-based traditional optimization algorithms are relatively mature and have advantages like high computational efficiency and strong reliability. However, traditional optimization methods have critical limitations when applied to complex and difficult optimization problems because (i) they often require that the objective function is convex, continuous and differentiable and the feasible region is a convex set, and (ii) their ability to process non-deterministic information is poor.

Over the years, plenty of algorithms based on artificial intelligence, sociality of biological swarms, or the laws of natural phenomena have emerged and been proved to be good alternative tools for solving such complex problems. This type of optimization algorithms can be roughly divided into the following five categories: (i) Evolutionary algorithms (EAs); (ii) swarm intelligence; (iii) simulated annealing [1]; (iv) tabu search [2,3]; and (v) neural networks. EAs include genetic algorithms (GA) [4,5], differential evolution [6], and immune system [7]. Among these three algorithms, GA is based on the concept of survival of the fittest mentioned in Darwin's theory of evolution. GA and DE can be considered as the most standard form of EAs. The swarm intelligence algorithms include classic particle swarm optimization (PSO) [8], bat algorithm [9], artificial bee colony [10], ant colony algorithm [11], firefly algorithm [12], artificial fish-swarm algorithm [13], fruit fly optimization algorithm [14], and so on. These algorithms mentioned above are based on social activities of birds, bats, honey bees, ants, fireflies, fish, and fruit flies, respectively. They are far less perfect in theory than the traditional optimization algorithms at present, and often fail to ensure the optimality of the solution. However, considering the perspective of practical applications, this kind of budding algorithms generally do not require the continuity and convexity of the objective function and constraints, and they also have excellent ability to adapt to data uncertainty.

The dragonfly algorithm (DA) is a new swarm intelligence optimization algorithm that was proposed by Mirjalili [15] in 2015. It is inspired by two unique clusters of dragonflies found in nature: Foraging groups (also known as static groups) and migratory groups (also known as dynamic groups). These two group behaviors of dragonflies are very similar to the two terms of group intelligence (global search and local development). In the static group, dragonflies will be divided into several sub-dragonfly groups to fly in different areas, which is the main target of the global search. In the dynamic group, dragonflies will gather into a large group and fly in one direction, which is advantageous for the local development. Since the principle of DA is simple, easy to implement, and possesses good optimization capabilities, it has shown promising results when applied to multi-objective optimization [15], image segmentation problem [16], and parameter optimization of support vector machines [17]. Moreover, DA has also been successfully applied to the accurate prediction model of power load [18], power system voltage stability evaluation [19], power flow management of smart grid system [20], economic dispatch [21], synthesis of concentric circular antenna arrays [22], and traveling salesman problem [23]. Further, based on a large number of numerical tests, Mirjalili proved that DA performs better than GA [4,5] and PSO [8].

It must be noted that DA was used to solve the continuous optimization problem, while many optimization problems have existed in binary search spaces. This suggests that the continuous version of the optimization algorithm can no longer meet the requirements of the binary optimization problems. A binary version of DA(BDA) was proposed by Mirjalili et al. [15] and successfully applied to the feature selection problems [24]. Like binary PSO (BPSO) [25] and binary BA [26], BDA used a transfer function to map the continuous search space into binary space. In [27], Hammouri et al. proposed three improved versions of BDA, named Linear-BDA, Quadratic-BDA, and Sinusoidal-BDA, for feature selection. By using different strategies to update main coefficients of the dragonfly algorithm, the three algorithms outperform the original BDA. However, such binary algorithms were still developed by using transfer functions, which may be limited in some high-dimensional optimization problems owing to slow convergence speed and poor algorithm stability.

To avoid such problems, intelligent optimization algorithms based on the angle modulation technique, originated in signal processing [28], were proposed recently such as angle modulated PSO [29], angle modulated DE [30], and angle modulated bat algorithm [31]. Inspired by these algorithms, an angle modulated dragonfly algorithm (AMDA) is proposed in this paper to make DA work more efficiently in binary-valued optimization spaces. By using a trigonometric function with four coefficients to generate n-dimensional bit strings, AMDA is observed from the experiments on benchmark functions and 0-1 knapsack problems to have better performance as compared to other optimization algorithms such as BPSO and BDA. Further, by adding a control coefficient to adjust the vertical displacement of the cosine part of the generating function, an improved angle modulated dragonfly algorithm (IAMDA) is proposed to enhance convergence performance and algorithm stability.

The rest of this paper is arranged as follows. The standard DA and the binary DA (BDA) are elaborated in Section 2. In Section 3, the proposed AMDA and IAMDA are explained. Further, Section 4 presents the analysis of the experimental results on 13 benchmark test functions and 12 0-1 knapsack problems. Finally, Section 5 discusses and concludes the performance of IAMDA with respect to BPSO, BDA, and AMDA.

2. Background

The dragonfly algorithm (DA) is a budding algorithm inspired by the social behavior of dragonflies, and this section gives a brief introduction about DA and its binary version.

2.1. The Dragonfly Algorithm

The dragonfly algorithm is an advanced swarm-based algorithm inspired by the static and dynamic clustering behaviors of dragonflies in nature. By simulating the behaviors of dragonflies looking for prey, mathematical modeling of the algorithm is done. During the modeling, the life habits of dragonflies, such as finding food, avoiding natural enemies, and choosing the flight routes are considered. The dragonfly population is divided into two groups: migratory swarm (also known as a dynamic swarm) and feeding swarm (also known as a static swarm). A large number of dragonfly clusters migrate in a common orientation for long distances intending to seek a better living environment in the dynamic swarm whereas, in a static swarm, each group is composed of a small group of dragonflies that fly back and forth in a small area to find other flying prey. The migration and feeding behaviors of dragonflies can be regarded as two main phases in meta-heuristics algorithm optimization: exploitation and exploration. Dragonflies gather into a large group and fly in one direction in a dynamic swarm, which is beneficial in the exploitation phase. In a static swarm, however, to find other flying prey, small groups of dragonflies fly back and forth in a small range, which is beneficial to the exploration of search agents. The dynamic and static groups of dragonflies proposed by Mirjalili [15] are demonstrated in Figure 1.

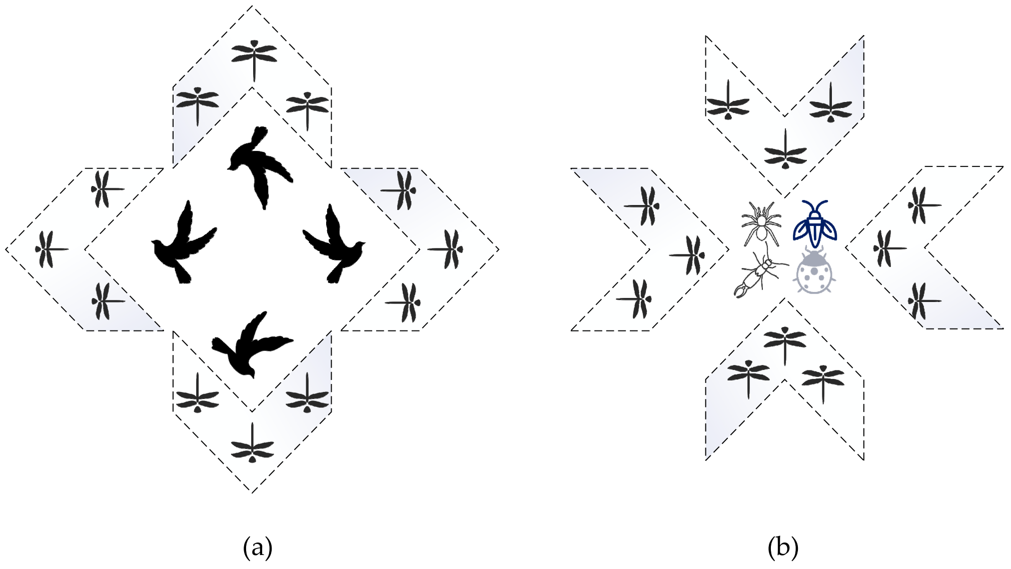

Figure 1. Dynamic swarms (**a**) versus static swarms (**b**).

Separation, alignment, and cohesion are three main principles in the insect swarms introduced by Reynolds [32] in 1987. The degree of separation refers to the static collision avoidance of the individuals from other individuals in the neighborhood, the degree of alignment indicates the velocity matching of individuals to that of other individuals in the neighborhood, and the degree of cohesion reflects the tendency of individuals toward the center of the mass of the neighborhood.

Every swarm in DA follows the principle of survival, and each dragonfly exhibits two separate behaviors: looking for food and avoiding the enemies in the surrounding. The positioning movement of dragonflies consists of the following five behaviors:

(1) Separation. The separation between two adjacent dragonflies is calculated as follows:

$$\boldsymbol{S}_i = -\sum_{j=1}^{N} (\boldsymbol{X}_i - \boldsymbol{X}_j) \tag{1}$$

where $\boldsymbol{S}_i$ is the separation of the *i-th* individual, $\boldsymbol{X}_i$ is the location of the *i-th* individual, $\boldsymbol{X}_j$ indicates the location of the *j-th* neighboring individual, and N is the number of neighborhoods.

(2) Alignment. The alignment of dragonflies is calculated as follows:

$$\boldsymbol{A}_i = \frac{\sum_{j=1}^{N} \boldsymbol{V}_j}{N} \tag{2}$$

where $\boldsymbol{A}_i$ indicates the alignment of *i-th* individual, $\boldsymbol{V}_j$ indicates the velocity of the *j-th* neighboring individual, and N is the number of neighborhoods.

(3) Cohesion. The cohesion is derived as follows:

$$\boldsymbol{C}_i = \frac{\sum_{j=1}^{N} \boldsymbol{X}_j}{N} - \boldsymbol{X}_i \tag{3}$$

where $\boldsymbol{C}_i$ indicates the cohesion of the *i-th* individual, $\boldsymbol{X}_i$ is the position of the *i-th* individual, N represents the number of neighboring individuals, and $\boldsymbol{X}_j$ shows the location of the *j-th* neighboring individual.

(4) Attraction. The attraction toward the source of food is calculated as follows:

$$\boldsymbol{F}_i = \boldsymbol{X}^{+} - \boldsymbol{X}_i \tag{4}$$

where $\boldsymbol{F}_i$ shows the food source of the *i-th* individual, $\boldsymbol{X}_i$ indicates the location of the *i-th* individual, and $\boldsymbol{X}^{+}$ represents the location of the food source.

(5) Distraction. The distraction from an enemy is derived as follows:

$$\boldsymbol{E}_i = \boldsymbol{X}^{-} + \boldsymbol{X}_i \tag{5}$$

where $\boldsymbol{E}_i$ represents the position of an enemy of the *i-th* individual, $\boldsymbol{X}_i$ is the location of the *i-th* individual, and $\boldsymbol{X}^{-}$ indicates the location of the natural enemy.

The above five swarming behaviors in the positioning movement of dragonflies are pictorially demonstrated in Figure 2.

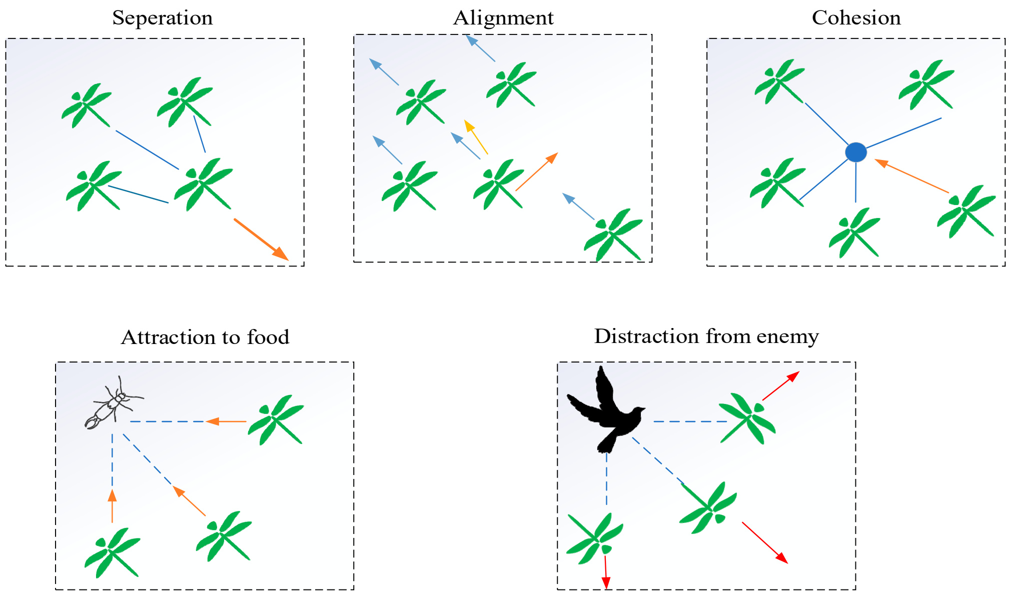

Figure 2. The five main social behaviors of dragonfly swarms.

To update the location of dragonflies in a search space and to simulate their movements, two vectors are considered: step vector ($\Delta \boldsymbol{X}$) and position vector ($\boldsymbol{X}$). The step vector suggests the direction of the movement of dragonflies and can be formally defined as follows:

$$\Delta \boldsymbol{X}_i^{t+1} = (s\boldsymbol{S}_i + a\boldsymbol{A}_i + c\boldsymbol{C}_i + f\boldsymbol{F}_i + e\boldsymbol{E}_i) + w\Delta \boldsymbol{X}_i^{t} \tag{6}$$

where s is the separation weight, $\boldsymbol{S}_i$ is the separation of the *i-th* individual, a shows the alignment weight, $\boldsymbol{A}_i$ indicates the alignment of *i-th* individual, c is the cohesion weight, $\boldsymbol{C}_i$ indicates the cohesion of the *i-th* individual, f represents the food factor, $\boldsymbol{F}_i$ shows the food source of the *i-th* individual, e indicates the enemy factor, $\boldsymbol{E}_i$ represents the position of an enemy of the *i-th* individual, w represents the inertia weight, and t represents the iteration count.

According to the calculation of the above step vector, the position vector can be updated by using Equation (7):

$$\boldsymbol{X}_i^{t+1} = \boldsymbol{X}_i^t + \Delta\boldsymbol{X}_i^{t+1} \tag{7}$$

If there are no neighboring solutions, the positon vectors are calculated by using the following equation:

$$\boldsymbol{X}_i^{t+1} = \boldsymbol{X}_i^t + Levy(dim) \times \boldsymbol{X}_i^t \tag{8}$$

where dim is the dimension of the position vector. Levy function can be described as follows:

$$Levy(dim) = 0.01 \times \frac{r_1 \times \sigma}{|r_2|^{\frac{1}{\beta}}} \tag{9}$$

where r_1 and r_2 are random numbers within [0,1], β is a constant, and:

$$\sigma = \left\{ \frac{\Gamma(1+\beta) \times \sin(\frac{\pi\beta}{2})}{\Gamma(\frac{1+\beta}{2}) \times \beta \times 2^{(\beta-1)/2}} \right\}^{\frac{1}{\beta}} \tag{10}$$

where $\Gamma(z) = (z-1)!$

The basic steps of DA can be summarized as the pseudo-codes highlighted in Figure 3.

Pseudo-code of DA

```
Initialize the dragonflies' population $X_i$ ($i$ = 1, 2, …, popsize)
Initialize the step vectors $\Delta X_i$ ($i$ = 1, 2, …, popsize)
while the end condition is not satisfied
  Calculate the objective values of all dragonflies
  Update the food source and enemy
  Update $w$, $s$, $a$, $c$, $f$, and $e$
  Calculate $S$, $A$, $C$, $F$, and $E$ using Equations (1)–(5)
  Update neighboring radius
  if a dragonfly has at least one neighboring dragonfly
    Update step vector using Equation (6)
    Update position vector using Equation (7)
  else
    Update position vector using Equation (8)
  end if
  Check and correct the new positions based on the boundaries of variables
end while
```

Figure 3. Pseudo-codes of DA.

2.2. *Binary Dragonfly Algorithm*

In the traditional DA, a search agent can easily change its position by introducing a step vector. However, in the discrete spaces, since a position vector can only be updated to 0 or 1, it is impossible to update a position vector according to the original method.

Mirjalili et al. [15] first proposed the binary dragonfly algorithm (BDA) to solve the binary optimization problems. BDA adopted the following transfer function to derive the probability of changing positions of all the search agents:

$$T(\Delta x) = \left| \frac{\Delta x}{\sqrt{\Delta x^2 + 1}} \right| \tag{11}$$

Further, the position vectors can be updated by the following formula:

$$\boldsymbol{X}_i^{t+1} = \begin{cases} \neg \boldsymbol{X}_i^t, r \leq T(\Delta x^{t+1}) \\ \boldsymbol{X}_i^t, r > (\Delta x^{t+1}) \end{cases} \tag{12}$$

where r is a random number between [0,1].

3. Improved Angle Modulated Dragonfly Algorithm (IAMDA)

3.1. AMDA

In this paper, the angle modulation technique is used for the homomorphic mapping of DA to convert the complex binary optimization problem into a simpler continuous problem. Different from the traditional BDA, the angle modulated dragonfly algorithm (AMDA) uses a trigonometric function to generate bit strings. The trigonometric function can be expressed as:

$$g(x) = sin(2\pi(x-a) \times b \times \cos(2\pi(x-a) \times c)) + d \tag{13}$$

where $x = 0, 1, \ldots, n_b - 1$, denotes the regular intervals at which the generating function is sampled, where n_b is the length of the required binary solution; the four coefficients (a, b, c, and d) are within [–1,1] at initialization. Then, the standard DA is used for evolving a quadruple composed of (a, b, c, d), and this leads each dragonfly to generate a position vector of the form $\boldsymbol{X}_i = (a, b, c, d)$. To evaluate a dragonfly, the coefficients from the dragonfly's current position are substituted into the generating function in Equation (13). Each sampled value at x is then mapped to a binary digit as follows:

$$g(x) = \begin{cases} 0, g(x) \leq 0 \\ 1, g(x) > 0 \end{cases} \tag{14}$$

The main steps of AMDA are simplified as the pseudo-code givens in Figure 4.

Pseudo-Code of AMDA

```
Initialize the continuous algorithm DA in $[-1,1]^4$
Initialize the dragonflies' population $X_i$ ($i$ = 1, 2, …, $popsize$)
Initialize the step vectors $\Delta X_i$ ($i$ = 1, 2, …, $popsize$)
while the end condition is not satisfied
    Calculate the objective values of all dragonflies
    Update the food source and enemy
    Update $w$, $s$, $a$, $c$, $f$, and $e$
    Calculate $S$, $A$, $C$, $F$, and $E$ using Equations (1)–(5)
    Calculate the output value $g(x)$ using Equation (13) to generate bit strings
    Update the position vectors using Equation (14)
end while
Return the best bit string as the solution;
```

Figure 4. Pseudo-codes of AMDA.

3.2. IAMDA

The prime advantage of AMDA is that it only needs four coefficients instead of the original n-dimensional bit strings. Thus, the computational cost will be significantly reduced. AMDA's generating function is a composite of a sine wave and a cosine wave. The vertical displacement of the sine wave can be controlled by the coefficient d in Equation (13) but the vertical displacement of the cosine wave cannot be corrected, which results in a large variance of the entire generating function value. In addition, if the initialization range of DA parameters is small, DA will encounter some difficulties while searching for a binary solution.

To alleviate the problem of the inability and control the vertical displacement of the cosine wave in the original generating function, this paper proposed an improved AMDA, called IAMDA. IAMDA uses one more coefficient k to control the degree of disturbance of the generating function in the mapping space:

$$g(x) = sin(2\pi(x-a) \times b \times \cos(2\pi(x-a) \times c) + k) + d \tag{15}$$

where the five coefficients (a, b, c, d, and k) are within $[-1{,}1]$ at initialization. The standard DA is used for evolving a quintuple composed of (a, b, c, d, k), and this led each dragonfly to generate a position vector of the form $\boldsymbol{X}_i = (a, b, c, d, k)$. To evaluate a dragonfly, the coefficients from the dragonfly's current position are substituted into Equation (15) and each sampled value is then mapped to a binary digit according to Equation (14).

In the original generating function, if the value of d is not large enough, the generating function will always be above or below 0, which will make the bit string only contain bit 0 or 1. Hence, a coefficient k is added to generate a bit string containing both 0 and 1 bits. The coefficient k is introduced to compensate for the insufficient disturbance in trigonometric function as well as to adjust vertical displacement of the cosine function. The comparison between the original and modified generating functions is presented in Figure 5. It can be observed from Figure 5 that the original generating function with the vertical displacement d = 0.2 is almost above 0. In this manner, it is easier to generate solutions that are mostly 0s or 1s. In the modified generating function, the displacement coefficient k increases the diversity of the solutions so that IAMDA may achieve better solutions even if the vertical displacement d is not large enough.

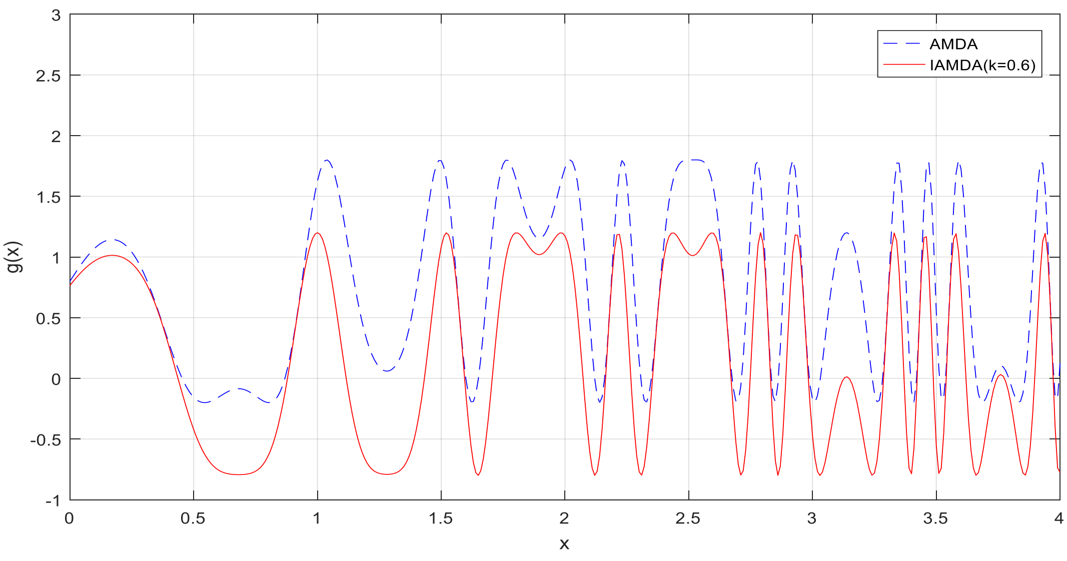

Figure 5. The original and modified generating functions. (a = 0, b = 0.5, c = 0.8, d = 0.2).

In order to demonstrate the mapping procedure, Figure 6 shows the procedure of using the modified trigonometric function to map a continuous five-dimensional search space into an n-dimensional binary search space. The main procedures of IAMDA are described as the following pseudo-codes given in Figure 7.

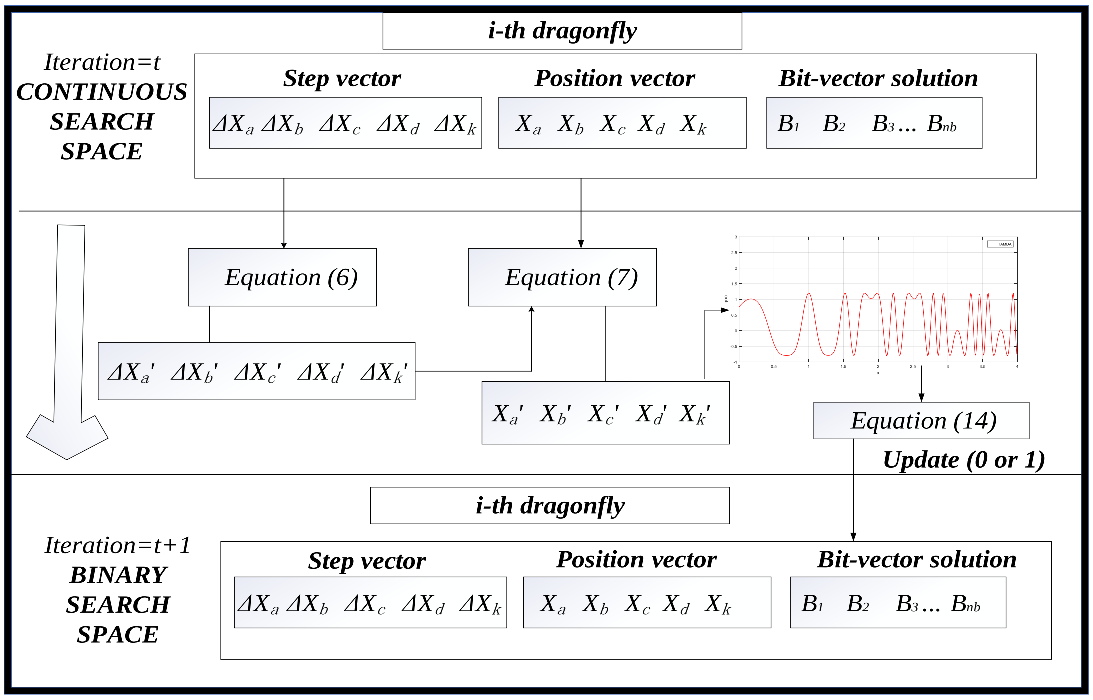

Figure 6. The process of mapping a continuous five-dimensional search space to an n-dimensional binary search space.

Pseudo-code of IAMDA

```
Initialize the continuous algorithm DA in $[-1,1]^5$
Initialize the dragonflies' population $X_i$ ($i = 1, 2, \ldots, popsize$)
Initialize the step vectors $\Delta X_i$ ($i = 1, 2, \ldots, popsize$)
while the end condition is not satisfied
    Calculate the objective values of all dragonflies
    Update the food source and enemy
    Update $w$, $s$, $a$, $c$, $f$, and $e$
    Calculate $S$, $A$, $C$, $F$, and $E$ using Equations (1)–(5)
    Calculate the output value $g(x)$ using Equation (13) to generate bit strings
    Update the position vectors using Equation (14)
end while
Return the best bit string as the solution;
```

Figure 7. Pseudo-codes of IAMDA.

4. Experimental Results and Discussion

4.1. Test Functions and Parameter Settings

To verify the performance and stability of IAMDA, two sets of benchmark test functions and 0-1 knapsack problems are selected. To efficiently compare the performance of each algorithm, the original AMDA, the basic BDA [15], and the BPSO [25] were selected to deal with the test problems. The average solution, median, and standard deviation are taken into consideration to evaluate each algorithm.

In this paper, the population size of IAMDA, AMDA, BDA, and BPSO is set to be 30 [15,33,34] and the number of iterations is set to be 500. Other parameter settings are listed in Table 1. To avoid the resulting bias caused by chance, the algorithms run independently on each function 30 times. Moreover, in this paper, each continuous variable is represented by 15 bits in binary. It should be noted that in order to indicate the sign of each functions' variable, one bit should be reserved. Hence, the dimension of each dragonfly, that is, the dimension of each generated bit string can be calculated as follows:

$$Dim_{dragonfly} = Dim_{function} \times 15 \tag{16}$$

where $Dim_{dragonfly}$ and $Dim_{function}$ represent the dimension of each dragonfly in IAMDA and the dimension of a specific benchmark function, respectively.

Table 1. Initial parameters of IAMDA, AMDA, BDA, and BPSO.

Algorithms	Parameters	Values
IAMDA	Number of dragonflies	30
	(a, b, c, d, k)	$[-1,1]$
	Max iteration	500
	Stopping criterion	Max iteration
AMDA	Number of dragonflies	30
	(a, b, c, d)	$[-1,1]$
	Max iteration	500
	Stopping criterion	Max iteration
BDA	Number of dragonflies	30
	Max iteration	500
	Stopping criterion	Max iteration
BPSO	Number of particles	30
	C_1, C_2	2
	w	Decreased linearly from 0.9 to 0.4
	Max velocity	0.6
	Max iteration	500
	Stopping criterion	Max iteration

Simulation environment: The processor is an Intel(R) Core (TM) i5-6500 2.40GHz, with 4.0GB RAM, Windows10 operating system, and the simulation software is Matlab2016a.

4.2. IAMDA Performance on Unimodal and Multimodal Benchmark Functions

The test functions are categorized into two groups: unimodal functions (f_1~f_7) and multimodal functions (f_8~f_{13}) [15,35,36]. To solve the optimal function, IAMDA is compared with several other algorithms on the 13 standard test functions. Each unimodal benchmark function has a single optimal value and it is easy to benchmark the convergence speed and optimization capability of an algorithm. On the contrary, multimodal benchmark functions have multiple optimal values, which makes them more complex as compared to unimodal functions. There is only one global optimal value among many optimal values, and an algorithm ought to avoid all local optimal approximations and tend to find the global optimal value. Hence, the multimodal test function can efficiently benchmark the exploration of the algorithm and the avoidance of local optima. The specific conditions about unimodal functions as well as multimodal functions are highlighted in Tables 2 and 3, respectively. Here, 'Function' indicates the test functions, 'n' represents the number of variables in the test function, 'Range' demonstrates the search scope of the test function, and 'f_{min}' indicates the global optimal value of the test function.

Figure 8 represents the convergence curves of the above four algorithms on different unimodal functions and Figure 9 shows the convergence curves of the above algorithms on various multimodal functions. Table 4 lists the average, median values, and standard deviation of IAMDA, AMDA BDA, and BPSO while testing the benchmark functions.

Table 2. Unimodal benchmark functions.

Function	Expression	n	Range	f_{min}
Sphere	$f_1(x) = \sum_{i=1}^{n} x_i$	5	[−100,100]	0
Schwefel 2.22	$f_2(x) = \sum_{i=1}^{n} \lvert x_i \rvert + \prod_{i=1}^{n} \lvert x_i \rvert$	5	[−10,10]	0
Schwefel 1.2	$f_3(x) = \sum_{i=1}^{n} (\sum_{j=1}^{i} x_j)^2$	5	[−100,100]	0
Schwefel 2.21	$f_4(x) = \{\lvert x_i \rvert, 1 \le i \le n\}$	5	[−100,100]	0
Rosenbrock	$f_5(x) = \sum_{i=1}^{n-1} [100(x_{i+1} - x_i{}^2) + (x_i - 1)^2]$	5	[−30,30]	0
Step	$f_6(x) = \sum_{i=1}^{n} ([x_i + 0.5])^2$	5	[−100,100]	0
Quartic	$f_7(x) = ix_i{}^4 + random[0, 1)$	5	[−1.28,1.28]	0

Table 3. Multimodal benchmark functions.

Function	Expression	n	Range	f_{min}
Schwefel	$f_8(x) = \sum_{i=1}^{n} -x_i \sin(\sqrt{\lvert x_i \rvert})$	5	[−500,500]	−418.9829 × 5
Rastrigrin	$f_9(x) = \sum_{i=1}^{n} [x_i{}^2 - 10\cos(2\pi x_i) + 10]$	5	[−5.12,5.12]	0
Ackley	$f_{10}(x) = -20\exp(-0.2\sqrt{\frac{1}{n}\sum_{i=1}^{n} x_i{}^2})$ $- \exp(\frac{1}{n}\sum_{i=1}^{n} \cos(2\pi x_i)) + 20 + e$	5	[−32.32]	0
Griewank	$f_{11}(x) = \frac{1}{4000}\sum_{i=1}^{n} x_i{}^2$ $-\prod_{i=1}^{n} \cos(\frac{x_i}{\sqrt{i}}) + 1$	5	[−600,600]	0
Penalty#	$f_{12}(x) = \frac{\pi}{n}\Big\{10\sin(\pi y_1) + \sum_{i=1}^{n-1} (y_i - 1)^2[1$ $+ \sin(\pi y_i + 1)] + (y_n - 1)^2\Big\}$ $+\sum_{i=1}^{n} u(x_i, 10, 100, 4)\}$ $yi = 1 + \frac{x_i+1}{4}$ $u(x_i, a, k, m) = \begin{cases} k(x_i - a)^m, x_i > a \\ 0, -a < x_i < a \\ k(-x_i - a)^m, x_i < -a \end{cases}$	5	[−50,50]	0
Penalized 1.2	$f_{13}(x) = 0.1\{\sin^2(3\pi x_1) + \sum_{i=1}^{n} (x_i - 1)^2[1$ $+ \sin^2(3\pi x_i + 1)] + (x_n - 1)^2[1 + \sin^2(2\pi x_n)]\Big\}$ $+\sum_{i=1}^{n} u(x_i, 5, 100, 4)$	5	[−50,50]	0

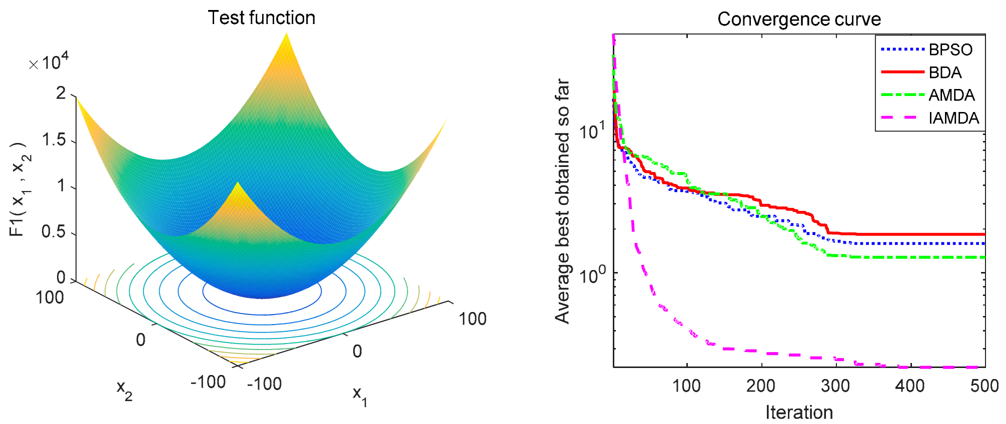

(a)

Figure 8. *Cont.*

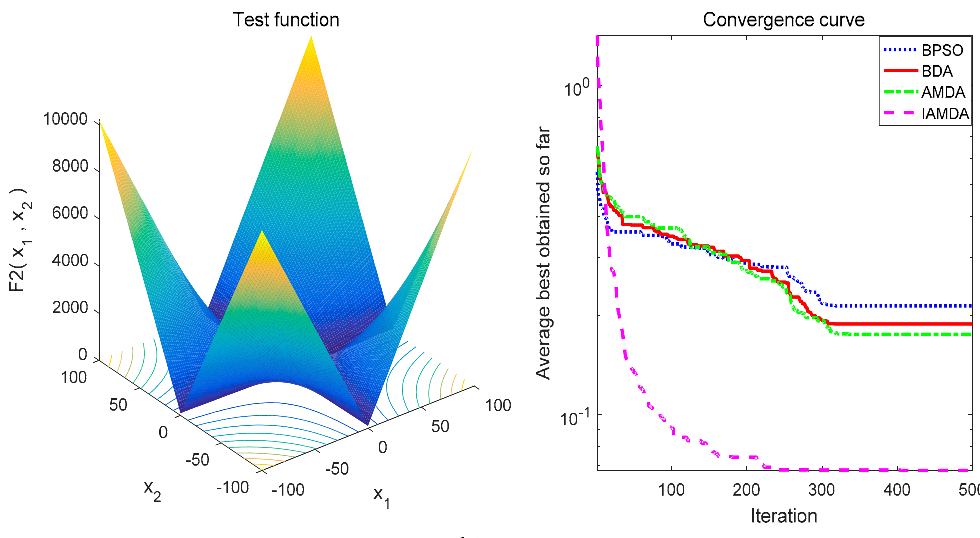

(**b**)

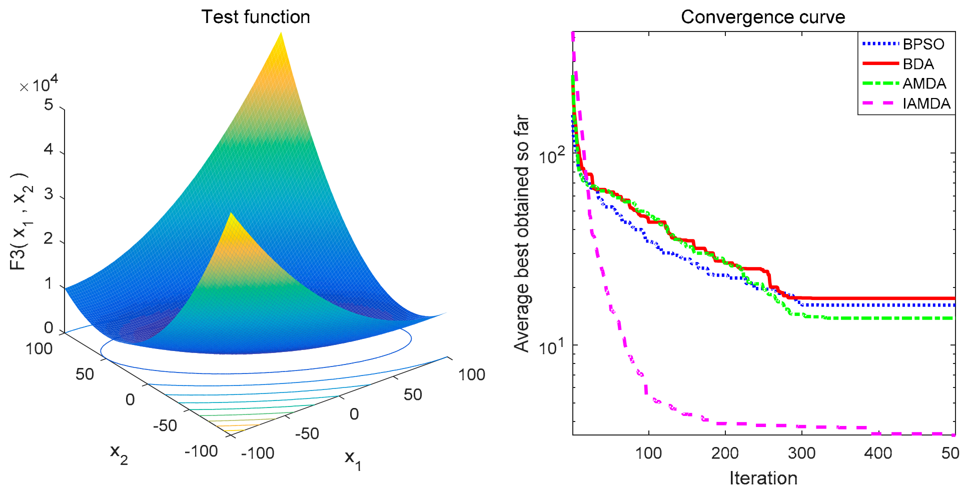

(**c**)

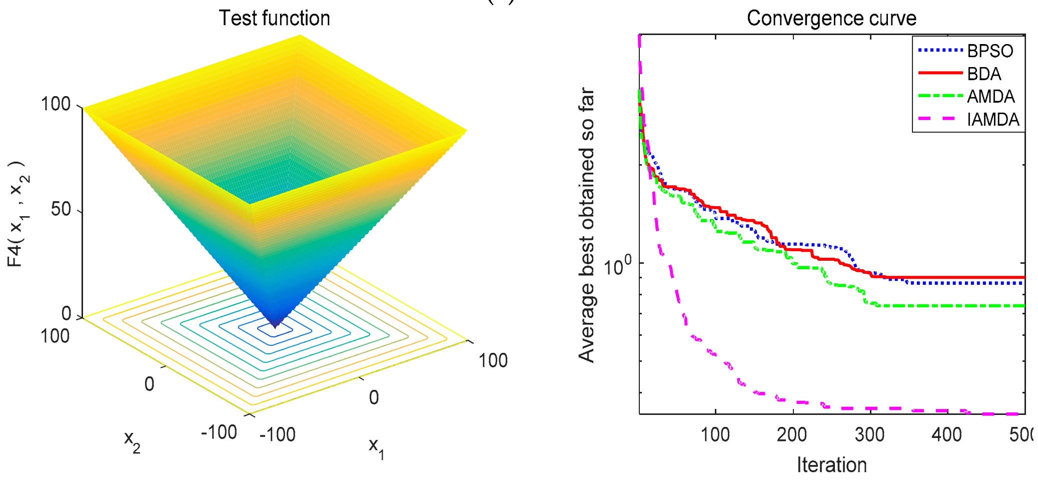

(**d**)

Figure 8. *Cont.*

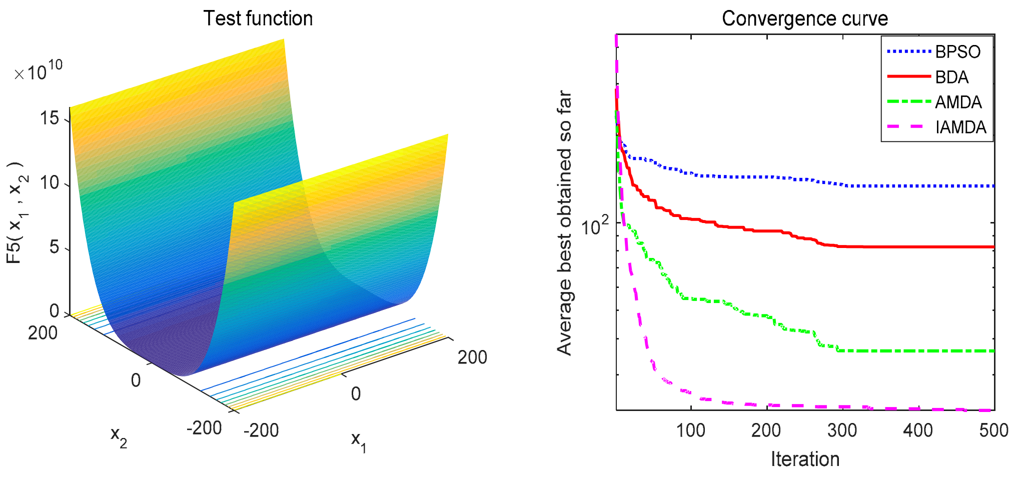

(e)

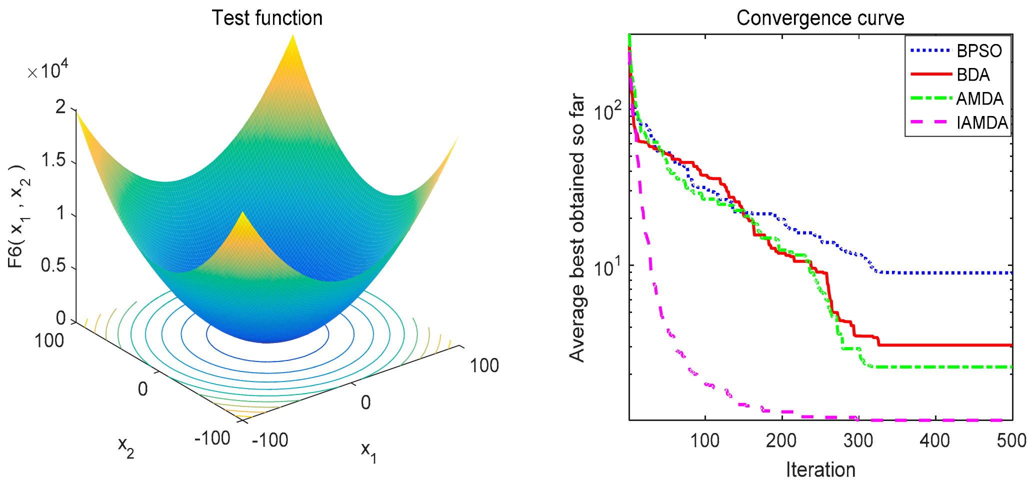

(f)

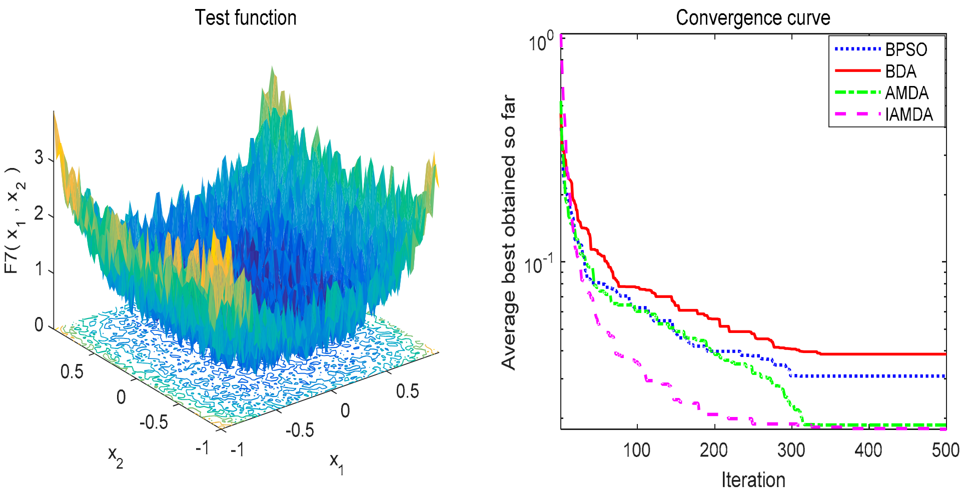

(g)

Figure 8. Convergence curve of IAMDA, AMDA, BDA, and BPSO on unimodal functions. (**a**) f_1. (**b**) f_2. (**c**) f_3. (**d**) f_4. (**e**) f_5. (**f**) f_6. (**g**) f_7.

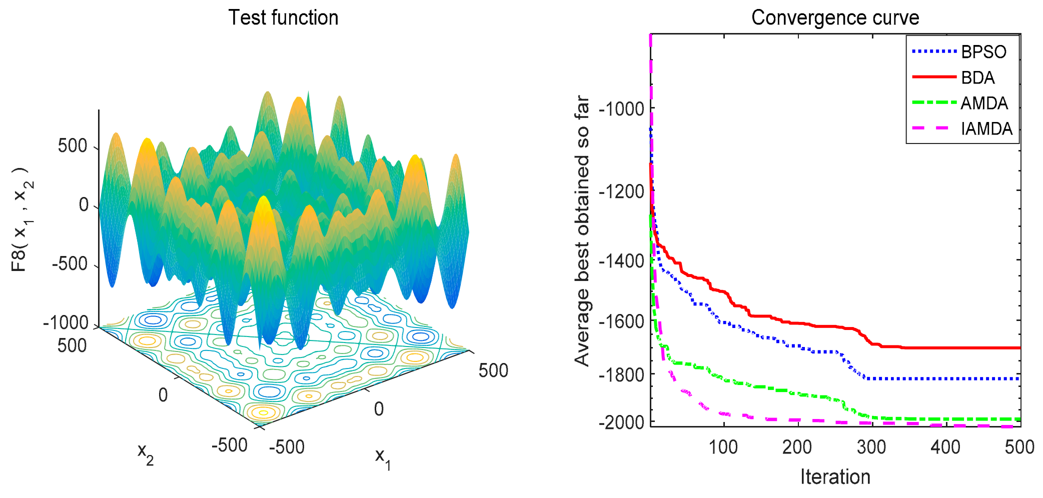

(**a**)

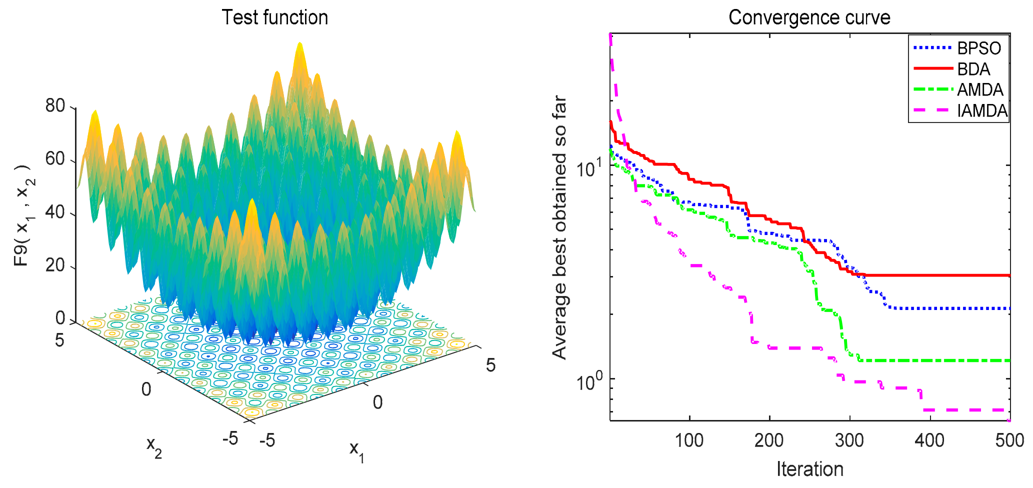

(**b**)

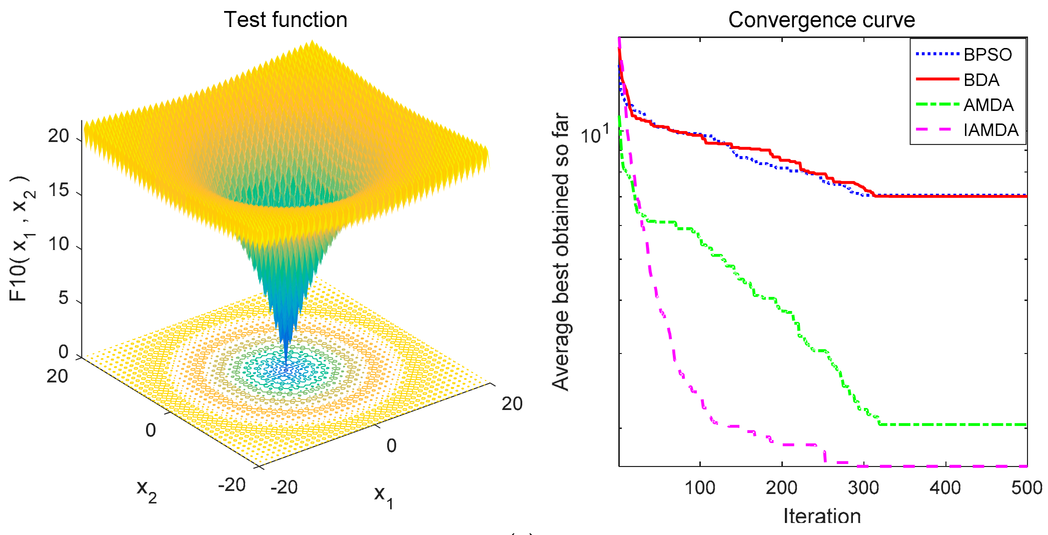

(**c**)

Figure 9. *Cont.*

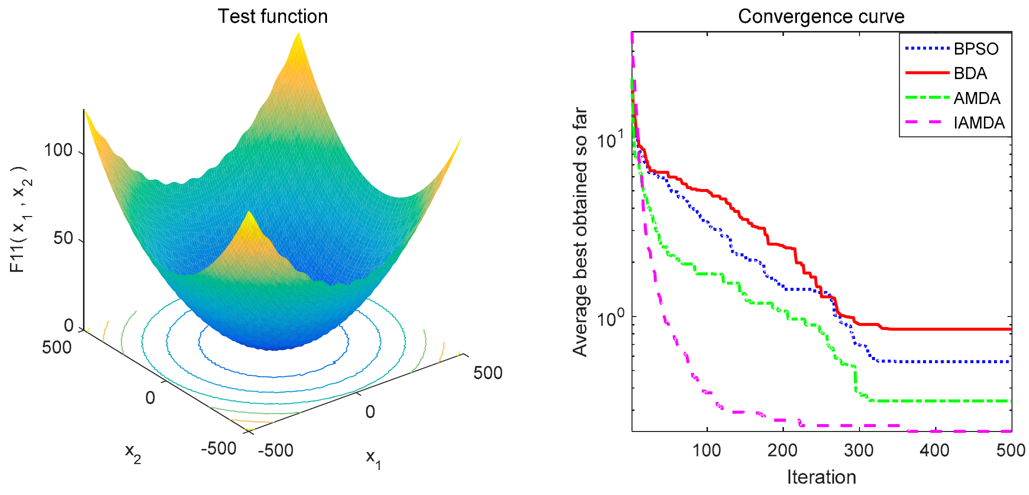

(**d**)

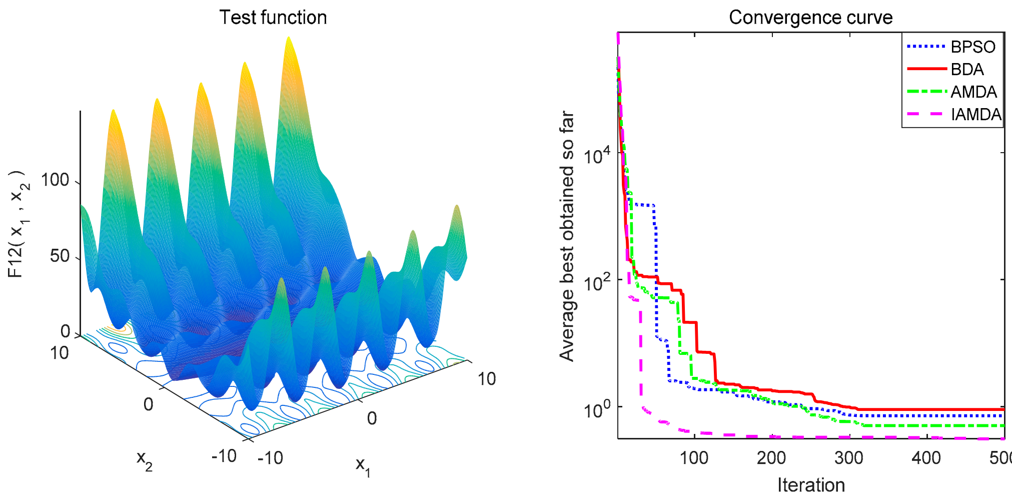

(**e**)

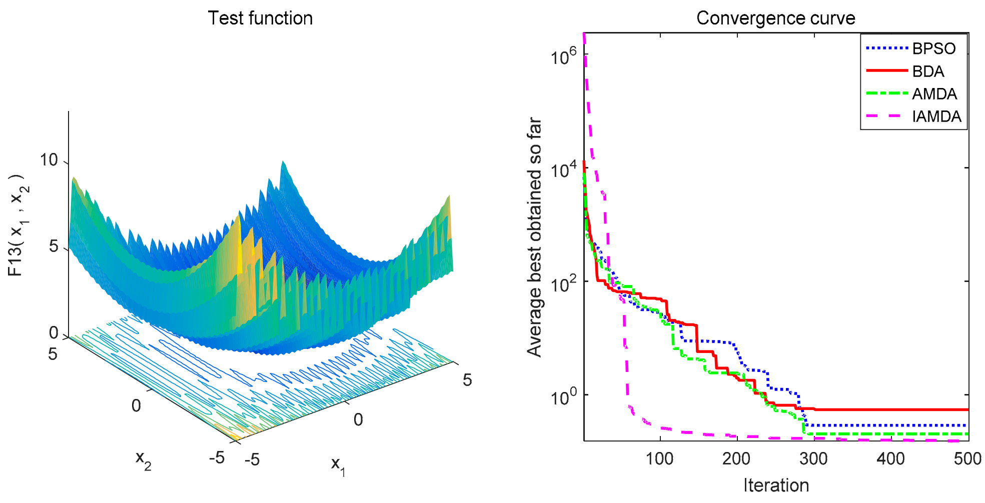

(**f**)

Figure 9. Convergence curve of IAMDA, AMDA, BDA, and BPSO on multimodal functions. (**a**) f_8. (**b**) f_9. (**c**) f_{10}. (**d**) f_{11}. (**e**) f_{12}. (**f**) f_{13}.

Table 4. Performance comparison among IAMDA, AMDA, BDA, and BPSO on unimodal benchmark functions and multimodal benchmark functions.

f	Metric	IAMDA	AMDA	BDA	BPSO
f_1	Mean	**0.2244**	1.2797	1.8412	1.5942
	SD	**0.1599**	0.9732	1.6625	1.3609
	Med	**0.1510**	0.6655	1.6669	1.3278
	Rank	1	2	4	3
f_2	Mean	**0.0676**	0.1751	0.1883	0.2137
	SD	**0.0216**	0.0913	0.1004	0.0882
	Med	**0.0585**	0.1423	0.2765	0.2702
	Rank	1	2	3	4
f_3	Mean	**3.4279**	15.1108	19.8865	21.8408
	SD	**1.9467**	14.1566	22.7839	11.6904
	Med	**2.4599**	18.7306	19.1034	23.0999
	Rank	1	2	3	4
f_4	Mean	**0.3383**	0.6840	0.8205	0.8701
	SD	**0.0988**	0.4461	0.3266	0.3559
	Med	**0.3446**	0.6906	0.9330	0.9568
	Rank	1	2	3	4
f_5	Mean	**22.6485**	36.2572	82.5599	133.7547
	SD	**3.0791**	10.9330	11.4133	9.5546
	Med	**20.4659**	30.0536	71.9376	124.0569
	Rank	1	2	3	4
f_6	Mean	**1.0166**	2.2309	3.0771	8.9318
	SD	**0.5524**	11.0604	9.7121	13.7554
	Med	**1.7111**	3.6660	3.1051	11.9169
	Rank	1	2	3	4
f_7	Mean	**0.0179**	0.0186	0.0387	0.0309
	SD	**0.0119**	0.0156	0.0235	0.0216
	Med	**0.0163**	0.0182	0.0327	0.0335
	Rank	1	2	4	3
f_8	Mean	**−2.0236e+03**	−1.9898e+03	−1.7002e+03	−1.8200e+03
	SD	**53.4828**	170.8601	147.8324	101.7015
	Med	**−2.0207e+03**	−1.8977e+03	−1.6972e+03	−1.8307e+03
	Rank	1	2	4	3
f_9	Mean	**0.6359**	1.2144	3.0472	2.1303
	SD	**1.7575**	5.5272	3.7159	5.0115
	Med	**0.7802**	0.8932	3.5783	2.3890
	Rank	1	2	4	3
f_{10}	Mean	**1.6269**	2.0406	7.0218	7.0607
	SD	**0.7271**	2.4153	2.5491	2.4290
	Med	**1.4469**	2.3801	6.7427	7.4276
	Rank	1	2	3	4
f_{11}	Mean	**0.2291**	0.3381	0.8498	0.5594
	SD	**0.2448**	1.2435	1.6054	1.1212
	Med	**0.2821**	0.4894	0.7234	0.4527
	Rank	1	2	4	3
f_{12}	Mean	**0.3092**	0.5014	0.8959	0.7153
	SD	**0.1880**	0.3313	0.5359	0.4502
	Med	**0.3947**	0.4381	0.8416	0.7652
	Rank	1	2	4	3
f_{13}	Mean	**0.1547**	0.2057	0.5492	0.2908
	SD	**0.0675**	0.7528	2.2227	1.2097
	Med	**0.1654**	0.2089	0.5847	0.1755
	Rank	1	2	4	3

Figures 8 and 9, respectively, represent the average convergence curves of the four algorithms on 7 unimodal functions and 6 multimodal functions after performing 30 experiments. The convergence curves in Figures 8 and 9 indicate that the convergence speed of IAMDA is significantly faster than that of the other three algorithms. For example, from Figure 8e, Figure 9a,e,f, it can be observed that the convergence of IAMDA can reach the optimal value at about 100 iterations.

In order to test whether IAMDA is statistically significant compared to other algorithms, statistical student's *t*-test [37] has been performed. The *t* value can be calculated by the following formula:

$$t = \frac{\overline{X_1} - \overline{X_2}}{\sqrt{(SD_1^2/(n_1-1)) + (SD_2^2/(n_2-1))}} \tag{17}$$

where $\overline{X_1}$, SD_1, and n_1 represent the mean value, standard deviation, and size of the first sample (AMDA, or BDA, or BPSO), respectively; $\overline{X_2}$, SD_2, and n_2 indicate the mean value, standard deviation, and size of the second sample (IAMDA), respectively. In this work, n_1 = n_2 = $Dim_{dragonfly}$. The positive *t* value means that IAMDA has better solutions compared to AMDA (or BDA or BPSO). The negative *t* value means that AMDA (or BDA or BPSO) produced better solutions than IAMDA. In our study, the confidence interval has been set at 95% which indicates $t_{0.05}$ = 1.96. When t > 1.96, the difference between two samples is significant and IAMDA is superior to AMDA (or BDA or BPSO). When $t < -1.96$, AMDA (or BDA or BPSO) is superior to IAMDA.

The *t* values calculated by Equation (17) over the selected 13 benchmark functions are presented in Tables 5 and 6. In the presented tables, 'N.S.' represents 'Not Significant', which means that the compared algorithms do not differ from each other significantly.

Table 5. Results of *t*-test for IAMDA against other three algorithms on unimodal benchmark functions with 30 independent runs.

f	AMDA and IAMDA		BDA and IAMDA		BPSO and IAMDA	
	t	**Sig.**	***t***	**Sig.**	***t***	**Sig.**
f_1	9.2046	IAMDA	8.3274	IAMDA	8.5994	IAMDA
f_2	9.8566	IAMDA	10.1103	IAMDA	13.8404	IAMDA
f_3	7.0330	IAMDA	6.1916	IAMDA	13.3650	IAMDA
f_4	6.5086	IAMDA	12.1566	IAMDA	12.3855	IAMDA
f_5	10.3097	IAMDA	43.5972	IAMDA	95.2107	IAMDA
f_6	0.9433	N.S.	1.9721	IAMDA	4.9460	IAMDA
f_7	0.3069	N.S.	6.7927	IAMDA	4.5347	IAMDA

Table 6. Results of *t*-test for IAMDA against other three algorithms on multimodal benchmark functions with 30 independent runs.

f	AMDA and IAMDA		BDA and IAMDA		BPSO and IAMDA	
	t	**Sig.**	***t***	**Sig.**	***t***	**Sig.**
f_8	1.9640	IAMDA	17.6961	IAMDA	15.2422	IAMDA
f_9	0.8580	N.S.	5.0462	IAMDA	2.4206	IAMDA
f_{10}	1.4109	N.S.	17.5076	IAMDA	18.4356	IAMDA
f_{11}	0.7398	N.S.	3.2879	IAMDA	2.4759	IAMDA
f_{12}	4.3404	IAMDA	8.8868	IAMDA	7.1604	IAMDA
f_{13}	0.5805	N.S.	1.9661	IAMDA	2.9663	IAMDA

Note that all the data in Table 4 are average values over 30 experiments. From the experimental results in Table 4, it can be analyzed that as compared to AMDA, BDA, and BPSO, IAMDA has obvious advantages in the optimization results of the 13 standard test functions. Judging from Table 5, IAMDA can find the optimal solutions in most cases of unimodal functions, which means that IAMDA has better exploitation capability. Additionally, according to the t values calculated in Table 6, IAMDA and AMDA exhibit similar exploration capability and have better performance than BDA and BPSO on multimodal functions. In brief, IAMDA has better exploitation and exploration capability. This proves that the introduction of the coefficient k in the angle modulation mechanism is beneficial for improving the convergence accuracy of the algorithm. Hence, according to the average convergence curves in Figures 8 and 9, and test data in Tables 4–6, it can be concluded that IAMDA outperforms the AMDA, BDA, and BPSO.

4.3. Zero-One Knapsack Problems

The 0-1 knapsack problem is one of combinatorial optimization problems, which means the time complexity of solving the knapsack problem grows very fast as the scale of the problem grows. Because of its complexity, the 0-1 knapsack problem has extremely crucial applications in number theory research, along with certain practical applications like cryptography [38], project selection [39], and feature selection [40–42]. It is a procedure of giving n items, and each item has two attributes, namely weight w_{i} and profit p_i. Capacity C indicates the maximum weight of the knapsack, and x_i represents whether the items i can be included in the knapsack or not. The target of 0-1 knapsack problem is to maximize the profit of the items in the knapsack and make the overall weights less than or equal to the knapsack capacity. The zero-one problem can be mathematically modeled as follows [43]:

$$\max f(p) = \sum_{i=1}^{N} p_i x_i \tag{18}$$

$$s.t.\begin{cases} f(w) = \sum_{i=1}^{N} w_i x_i \le C \\ x_i = 0, 1 (i = 1, 2, \ldots, N) \end{cases} \tag{19}$$

Since the procedure of the 0-1 knapsack problem is essentially a binary optimization process, binary heuristic algorithms such as BPSO and BDA are required to solve the 0-1 knapsack problems. The following tables highlight 12 classic 0-1 knapsack problems, including five classic 0-1 knapsack problems k_1–k_5 [44] listed in Table 7 and seven high-dimensional 0-1 knapsack problems k_6–k_{12} [45] listed in Table 8. The larger the problem dimension, the greater the computational complexity and the longer the execution time. In the tables, 'D' indicates the dimension of a knapsack problem, 'w' and 'p' represent the weight and profit of each object, respectively. 'C' denotes the capacity of a knapsack, 'Opt' shows the optimal value and 'Total values' in Table 6 represents overall profits of all items. Table 9 shows the best, worst, and average solutions for 0-1 knapsack problems. Additionally, the average calculation time and the standard deviation (SD) are listed. Table 10 lists the p values of the Wilcoxon ranksum test over the seven high-dimensional knapsack problems, 'N.S.' represents 'not significant', which means that the compared algorithms do not differ from each other significantly.

Table 7. Related parameters of five classic 0-1 knapsack problems.

No.	D	Parameter (w, p, C)	Opt
k_1	10	w = (95,4,60,32,23,72,80,62,65,46); p = (55,10,47,5,4,50,8,61,85,87); C = 269	295
k_2	20	w = (92,4,43,83,84,68,92,82,6,44,32,18,56,83,25,96,70,48,14,58); p = (44,46,90,72,91,40,75,35,8,54,78,40,77,15,61,17,75,29,75,63); C = 878	1024

Table 7. *Cont.*

No.	D	Parameter (w, p, C)	Opt
k_3	50	w = (80,82,85,70,72,70,66,50,55,25,50,55,40,48,59,32,22,60,30, 32,40,38,35,32,25,28,30,22,50,30,45,30,60,50,20,65,20,25,30, 10,20,25,15,10,10,10,4,4,2,1); p = (220,208,198,192,180,180,165,162,160,158,155,130,125, 122,120,118,115,110,105,101,100,100,98,96,95,90,88,82,80,77,75,7,72,70,69,66,65,63,60,58,56,50,30,20,15, 0,8,5,3,1); C = 1000	3103
k_4	80	w = (40, 27,5,21,51, 16, 42, 18, 52, 28, 57, 34, 44, 43,52,55,53,42, 47, 56,57,44, 16,2, 12, 9, 40, 23, 56, 3, 39,16, 54, 36, 52,5,53, 48, 23, 47, 41, 49, 22, 42, 10, 16, 53, 58, 40, 1,43,56,40,32,44,35, 37, 45, 52, 56, 40, 2, 23,49, 50, 26, 11,35, 32, 34, 58, 6, 52,26,31, 23, 4, 52, 53, 19); p = (199,194,193,191,189,178,174,169,164,164,161,158,157, 154,152,152,149,142,131,125,124,124,124,122,119,116,114,113,111,110,109,100,97,94,91,82,82,81,80, 80,80,79,77,76,74, 72, 71, 70, 69,68, 65, 65, 61, 56, 55, 54, 53, 47, 47, 46, 41, 36, 34, 32, 32,30, 29, 29, 26, 25, 23, 22, 20, 11, 10, 9,5,4,3, 1); C = 1173	5183
k_5	100	w = (54, 95, 36, 18,4, 71,83, 16, 27, 84, 88, 45, 94, 64, 14, 80, 4, 23, 75, 36, 90, 20, 77, 32, 58, 6, 14, 86, 84, 59,71, 21, 30, 22, 96, 49, 81, 48, 37, 28, 6, 84,19,55,88,38,51,52,79,55,70,53,64,99,61,86,1,64,32,60,42,45,34,22,49,37,33,1,78,43,85,24,96,32,99,57, 23,8,10,74,59,89,95,40,46,65,6,89,84,83,6,19,45, 59, 26, 13, 8, 26, 5, 9); p = (297, 295, 293, 292, 291, 289, 284, 284, 283, 283, 281, 280, 279, 277, 276, 275, 273,264, 260, 257, 250, 236, 236, 235, 235, 233, 232, 232, 228, 218, 217, 214, 211, 208, 205, 204, 203, 201, 196, 194,193, 193, 192, 191, 190, 187, 187, 184, 184, 184, 181, 179, 176, 173, 172, 171, 160, 128, 123, 114, 113, 107, 105,101, 100, 100, 99, 98, 97, 94, 94, 93, 91, 80, 74, 73, 72, 63, 63, 62, 61, 60, 56, 53, 52, 50, 48, 46, 40, 40, 35, 28, 22,22, 18, 15, 12,11, 6,5); C = 3818;	15,170

Table 8. Related parameters of seven randomly generated zero-one knapsack problems.

No.	D	C	Total Values
k_6	200	1948.5	15,132
k_7	300	2793.5	22,498
k_8	500	4863.5	37,519
k_9	800	7440.5	59,791
k_{10}	1000	9543.5	75,603
k_{11}	1200	11,267	90,291
k_{12}	1500	14,335	111,466

Table 9. Result comparisons among IAMDA, AMDA, BDA, and BPSO on 0-1 knapsack problems.

No.	Alg.	Best	Worst	Mean	SD	Time
k_1	IAMDA	**295**	**295**	**295**	0	0.2175
	AMDA	**295**	**295**	**295**	0	0.2112
	BDA	**295**	**295**	**295**	0	0.9646
	BPSO	**295**	**295**	**295**	0	**0.0389**
k_2	IAMDA	**1024**	1018	1.0231e+03	2.1981	0.2858
	AMDA	**1024**	1013	1.0226e+03	3.5452	0.2766
	BDA	**1024**	1018	1.0225e+03	2.6656	1.0450
	BPSO	**1024**	**1024**	**1024**	**0**	**0.0618**
k_3	IAMDA	**3076**	**2991**	3.0308e+03	**21.1636**	0.2863
	AMDA	3064	2969	**3.0367e+03**	29.6729	0.2782
	BDA	3074	2970	3.0203e+03	30.0559	1.0461
	BPSO	3074	2957	2.9978e+03	26.6114	**0.1460**

Table 9. *Cont.*

No.	Alg.	Best	Worst	Mean	SD	Time
k_4	IAMDA	4991	**4763**	**4.9131e+03**	**66.2322**	0.3929
	AMDA	**5090**	4678	4.8918e+03	115.7004	0.3796
	BDA	5041	4705	4.8880e+03	105.7243	1.2035
	BPSO	4695	4348	4.4823e+03	99.1591	**0.2175**
k_5	IAMDA	14,965	**14,261**	**1.4631e+04**	**166.4238**	0.3979
	AMDA	**15,010**	14,155	1.4626e+04	220.8765	0.3803
	BDA	14,986	14,149	1.4611e+04	208.1295	1.2696
	BPSO	13,986	13,324	1.3595e+04	188.0612	**0.2488**
k_6	IAMDA	**1.3075e+04**	**1.2300e+04**	**1.2632e+04**	**207.7428**	0.4770
	AMDA	1.2801e+04	1.1921e+04	1.2498e+04	211.4083	**0.4631**
	BDA	1.2820e+04	1.1501e+04	1.2316e+04	315.2521	1.6793
	BPSO	1.1640e+04	1.0951e+04	1.1174e+04	213.5035	0.6185
k_7	IAMDA	**1.8386e+04**	**1.6408e+04**	**1.7800e+04**	413.3773	0.6500
	AMDA	1.8220e+04	1.6107e+04	1.7595e+04	594.7544	**0.6137**
	BDA	1.7979e+04	1.6227e+04	1.7554e+04	370.3743	2.8821
	BPSO	1.6084e+04	1.5385e+04	1.5717e+04	**181.8523**	0.8482
k_8	IAMDA	**3.1266e+04**	**2.8010e+04**	**3.0387e+04**	713.8203	0.9952
	AMDA	3.0763e+04	2.7902e+04	3.0134e+04	816.0871	**0.9457**
	BDA	2.9598e+04	2.6478e+04	2.8067e+04	848.2838	3.6978
	BPSO	2.5404e+04	2.3997e+04	2.4656e+04	**328.1345**	1.3125
k_9	IAMDA	**4.7364e+04**	**4.1702e+04**	**4.5928e+04**	1.4190e+03	1.7125
	AMDA	4.7078e+04	4.0453e+04	4.5502e+04	1.6564e+03	**1.7014**
	BDA	4.5734e+04	4.1055e+04	4.2988e+04	1.2721e+03	5.3235
	BPSO	3.8119e+04	3.6775e+04	3.7448e+04	**355.7410**	2.0791
k_{10}	IAMDA	**5.9952e+04**	5.5355e+04	5.8646e+04	1.3125e+03	2.5047
	AMDA	5.9566e+04	5.3099e+04	5.7783e+04	1.8917e+03	**2.5023**
	BDA	5.7356e+04	5.0011e+04	5.3727e+04	2.3538e+03	6.2211
	BPSO	4.6572e+04	4.5209e+04	4.5749e+04	**362.8049**	2.6863
k_{11}	IAMDA	**7.1022e+04**	**6.3479e+04**	**6.8977e+04**	1.9784e+03	3.2814
	AMDA	7.0417e+04	5.9200e+04	6.7161e+04	3.0546e+03	3.0616
	BDA	6.7241e+04	5.5492e+04	6.3396e+04	3.0978e+03	7.6517
	BPSO	5.5506e+04	5.3168e+04	5.4227e+04	**552.3881**	**3.0838**
k_{12}	IAMDA	**8.8872e+04**	**8.1067e+04**	**8.7179e+04**	2.1245e+03	3.5053
	AMDA	8.8691e+04	7.8917e+04	8.6422e+04	2.5499e+03	**3.3711**
	BDA	8.2644e+04	6.9772e+04	7.6970e+04	3.9042e+03	8.5147
	BPSO	6.7097e+04	6.5470e+04	6.6496e+04	**648.1773**	3.7690

Table 10. *p*-values of the Wilcoxon ranksum test on large-scale knapsack problems.

f	AMDA and IAMDA		BDA and IAMDA		BPSO and IAMDA	
	t	Sig.	t	Sig.	t	Sig.
k_6	0.0709	N.S.	0.0937	IAMDA	6.7956e-08	IAMDA
k_7	0.2085	N.S.	0.0066	IAMDA	6.7956e-08	IAMDA
k_8	0.3793	N.S.	4.5390e-07	IAMDA	6.7956e-08	IAMDA
k_9	0.2393	N.S.	5.8736e-07	IAMDA	6.7956e-08	IAMDA
k_{10}	0.0409	IAMDA	3.4156e-07	IAMDA	6.7956e-08	IAMDA
k_{11}	0.0155	IAMDA	2.6898e-06	IAMDA	6.7956e-08	IAMDA
k_{12}	0.1636	N.S.	1.2346e-07	IAMDA	6.7956e-08	IAMDA

Table 9 presents the test results of the four algorithms after performing 30 experiments. It can be observed that for k_1 and k_2, all the four algorithms can find the optimal solution. Whereas for k_3–k_{12}, IAMDA and AMDA can always find better results in less computation time, suggesting the strong global optimization capabilities and computational robustness of IAMDA and AMDA in binary spaces. Additionally, it can be observed that the higher the dimensionality of the 0-1 knapsack problem, the more obvious the advantages of IAMDA and AMDA. Moreover, as compared to AMDA, the standard deviation of IAMDA is much smaller, which suggests that IAMDA is more stable and effective than AMDA for solving the 0-1 knapsack problems. Besides, the p values listed in Table 10 prove that IAMDA and AMDA outperform BDA and BPSO in solving large-scale knapsack problems.

Figure 10 shows the average convergence curves of the four algorithms on the selected large-scale problems in 30 independent runs. As denoted in the figure, (i) the purple curve representing IAMDA is always on the top of the other curves and the effect becomes more obvious with the increasing problem dimension; (ii) the red and blue curves representing BDA and BPSO are slowly climbing, or even stagnating. In other words, IMADA has the strongest convergence, while BDA and BPSO converge prematurely to solve large-scale testing problems.

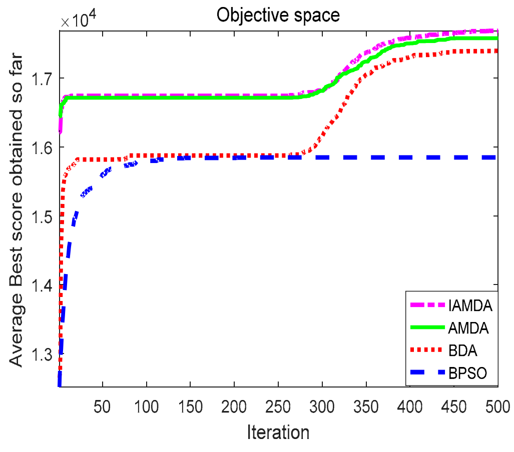

(**a**) k_7

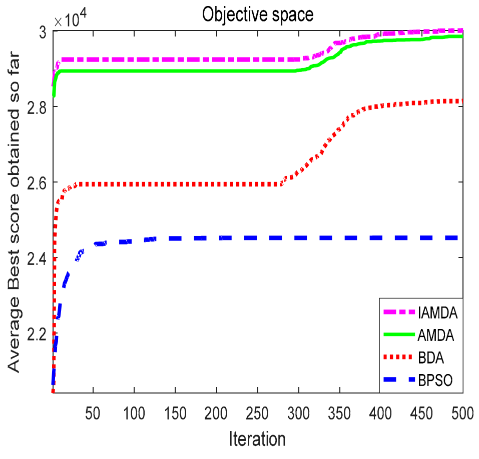

(**b**) k_8

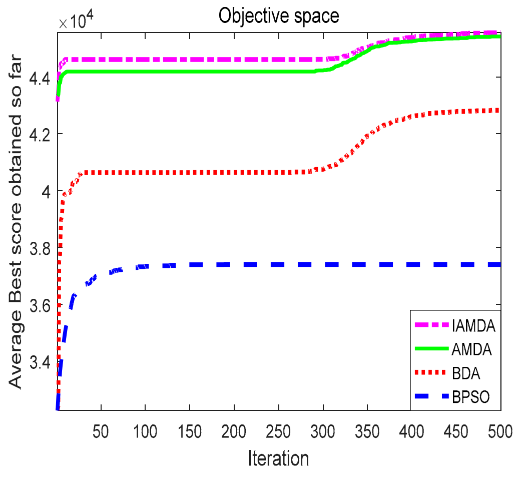

(**c**) k_9

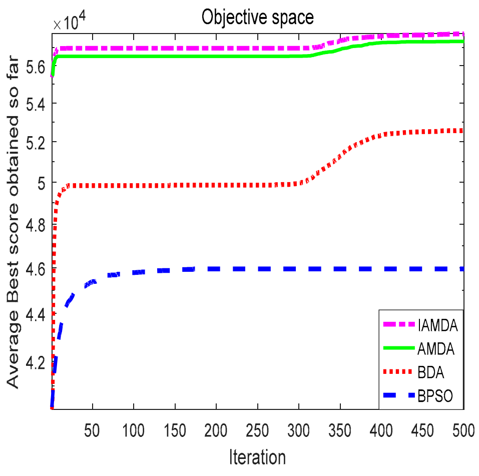

(**d**) k_{10}

Figure 10. *Cont.*

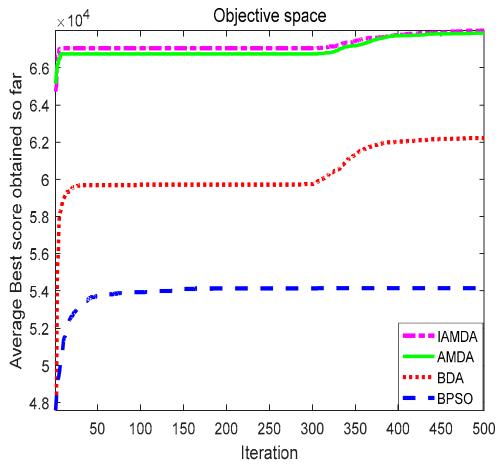

(**e**) k_{11}

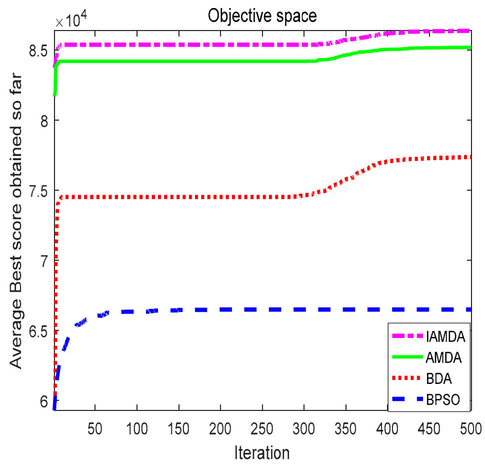

(**f**) k_{12}

Figure 10. Average convergence curves of IAMDA, AMDA, BDA, and BPSO on some selected large-scale problems over 30 independent runs: (**a**) k_7. (**b**) k_8. (**c**) k_9. (**d**) k_{10}. (**e**) k_{11}. (**f**) k_{12}.

Figure 11 depicts the distribution of the results of the knapsack problem obtained by the four algorithms. As shown in the figure, (i) the solution produced by IAMDA always give better results, and the results vary within a confined range, thus producing a smaller variance; (ii) diversity of the results produced by BDA is the best; and (iii) in the majority of the problems, many of the results produced by IAMDA are as applicable as those produced by AMDA; however, IAMDA has a smaller variance than AMDA.

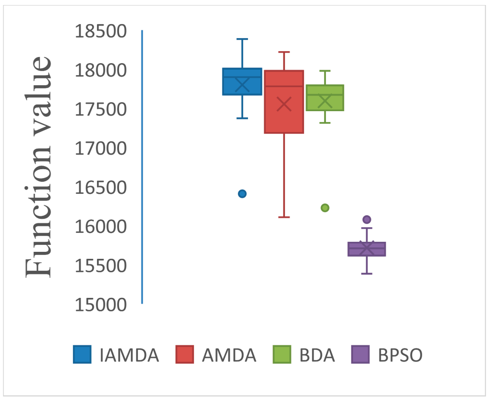

(**a**) k_7

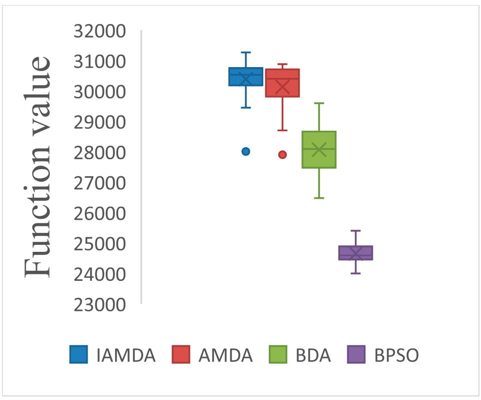

(**b**) k_8

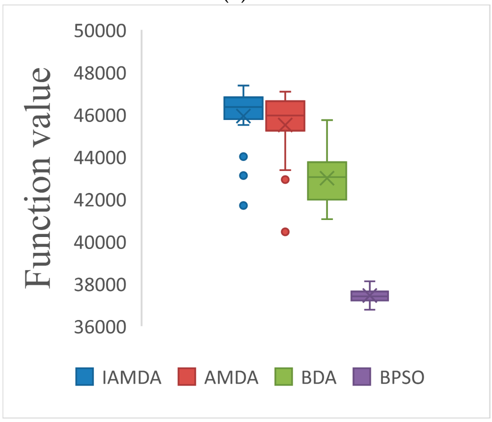

(**c**) k_9

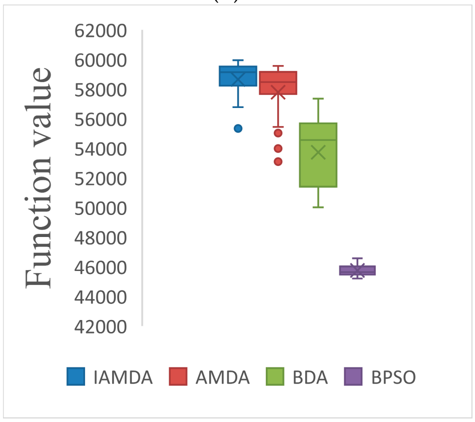

(**d**) k_{10}

Figure 11. *Cont.*

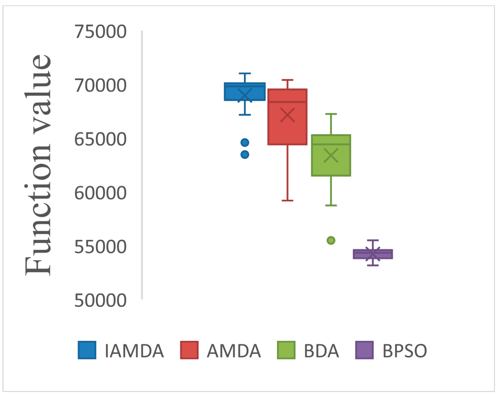

(**e**) k_{11}

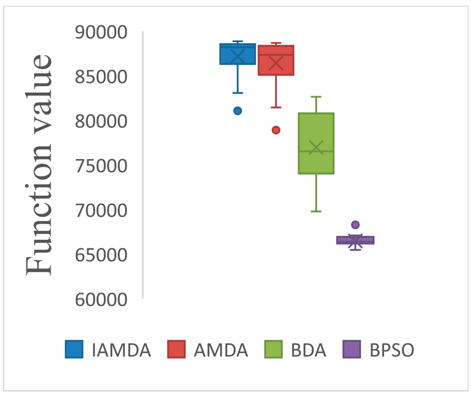

(**f**) k_{12}

Figure 11. The box plots of IAMDA, AMDA, BDA, and BPSO on some selected large-scale problems. (**a**) k_7. (**b**) k_8. (**c**) k_9. (**d**) k_{10}. (**e**) k_{11}. (**f**) k_{12}.

Figure 12 indicates the average computational time of the above algorithms on the selected k_1–k_{12} knapsack problems. It can be noted from the bar diagram that (i) the average computational time of AMDA is the least, and (ii) the computational time of IAMDA, AMDA, and BPSO are similar, and all are significantly less than the calculation time of BDA.

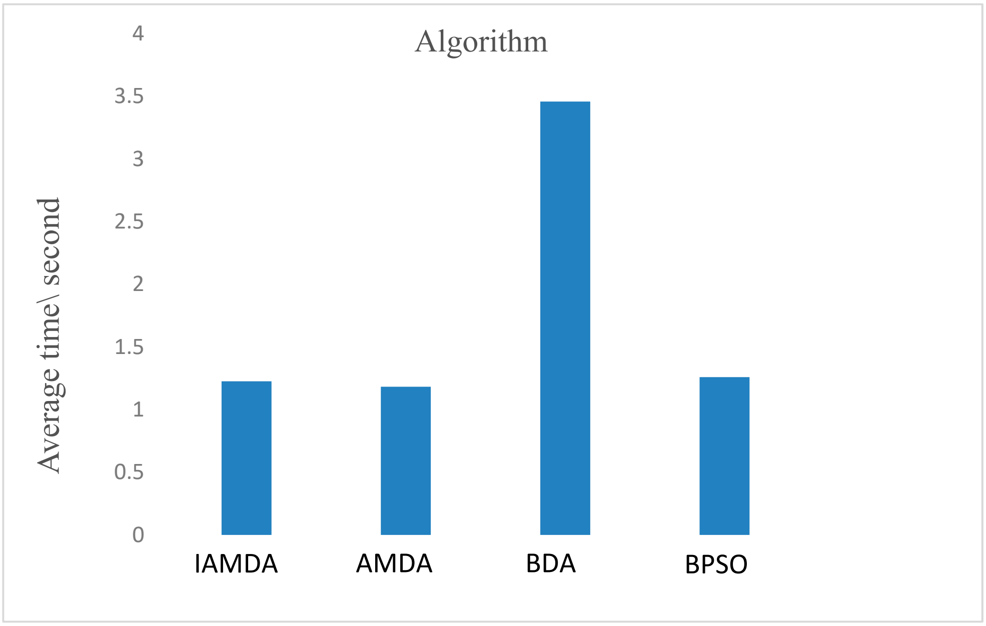

Figure 12. Average computational time of IAMDA, AMDA, BDA, and BPSO on some selected large-scale problems k_7–k_{12} over 30 independent runs.

It can be summarized from the above simulation results that when IAMDA solves the 0-1 knapsack problems, it decreases the computational time while ensuring the accuracy of the solution. IAMDA performs well on both low-dimensional as well as high-dimensional problems. Moreover, it has a smaller variance than AMDA and the original BDA, indicating better robustness of IAMDA.

5. Conclusions

To make the dragonfly algorithm work efficiently in the binary space, this paper applies an angle modulation mechanism to the dragonfly algorithm. AMDA uses the trigonometric function to generate bit strings corresponding to the binary problem solutions instead of directly running on the high-dimensional binary spaces. Thus, AMDA can significantly reduce the computational cost as compared to the traditional BDA using transfer functions. However, AMDA also has some limitations such as poor algorithm stability and slow convergence speed due to the lack of control on the vertical displacement of the cosine part in the generating function.

To deal with the limitations, this paper proposes an improved angle modulated dragonfly algorithm (IAMDA). Based on AMDA, one more coefficient is added to adjust the vertical displacement of the cosine part in the original generating function. From the test results of unimodal and multimodal benchmark functions and 12 low-dimensional and high-dimensional zero-one knapsack problems, it can be concluded that IAMDA outperforms AMDA, BDA, and BPSO in terms of stability, convergence rate, and quality of the solution. Additionally, it significantly reduces the computational time as compared to BDA. For future advancements, our studies may include multidimensional zero-one knapsack problems, multi-objective optimization problems, and so on. Furthermore, our research will be applied to practical applications such as feature selection and antenna topology optimization.

Author Contributions: Conceptualization: L.W. and J.D.; methodology: L.W. and J.D.; software: L.W. and R.S.; validation: L.W. and J.D.; investigation: L.W.; resources: J.D.; data curation: L.W. and J.D.; writing—original draft preparation: L.W.; writing—review and editing: R.S. and J.D.; visualization: L.W.; supervision: L.W. and J.D.; project administration: J.D.; funding acquisition: J.D. and R.S. All authors have read and agreed to the published version of the manuscript.

Funding: This research was funded in part by the National Natural Science Foundation of China, grant number 61801521 and 61971450, in part by the Natural Science Foundation of Hunan Province, grant number 2018JJ2533, and in part by the Fundamental Research Funds for the Central Universities, grant number 2018gczd014 and 20190038020050.

Data Availability Statement: Data is contained within the article.

Conflicts of Interest: The authors declare no conflict of interest.

References

1. Kirkpatrick, S.; Gelatt, C.D.; Vecchi, M.P. Optimization by simulated annealing. *Science* **1983**, *220*, 671–680. [CrossRef]
2. Glover, F. Tabu search—part I. *Orsa J. Comput.* **1989**, *1*, 190–206. [CrossRef]
3. Glover, F. Tabu search—part II. *Orsa J. Comput.* **1990**, *2*, 4–32. [CrossRef]
4. Sampson, J.R. *Adaptation in Natural and Artificial Systems (John H. Holland)*; Society for Industrial and Applied Mathematics: Philadelphia, PA, USA, 1975.
5. Mitchell, M. *An Introduction to Genetic Algorithm*; MIT press: Cambridge, MA, USA, 1998.
6. Das, S.; Suganthan, P.N. Differential evolution: A survey of the state-of-the-art. *IEEE Trans. Evol. Comput.* **2010**, *15*, 4–31. [CrossRef]
7. Farmer, J.D.; Packard, N.H.; Perelson, A.S. The immune system, adaptation, and machine learning. *Phys. D Nonlinear Phenom.* **1986**, *22*, 187–204. [CrossRef]
8. Kennedy, J.; Eberhart, R. Particle swarm optimization. In Proceedings of the ICNN'95-International Conference on Neural Networks, Perth, WA, Australia, 6 August 2002; pp. 1942–1948.
9. Yang, X.-S. *A New Metaheuristic Bat-Inspired Algorithm. Nature Inspired Cooperative Strategies for Optimization (NICSO 2010)*; Springer: Berlin/Heidelberg, Germany, 2010; pp. 65–74.
10. Liu, X.-F.; Zhan, Z.-H.; Deng, J.D.; Li, Y.; Gu, T.; Zhang, J. An energy efficient ant colony system for virtual machine placement in cloud computing. *IEEE Trans. Evol. Comput.* **2016**, *22*, 113–128. [CrossRef]
11. Chen, Z.-G.; Zhan, Z.-H.; Lin, Y.; Gong, Y.-J.; Gu, T.-L.; Zhao, F.; Yuan, H.-Q.; Chen, X.; Li, Q.; Zhang, J. Multiobjective cloud workflow scheduling: A multiple populations ant colony system approach. *IEEE Trans. Cybern.* **2018**, *49*, 2912–2926. [CrossRef]
12. Yang, X.-S. *Firefly Algorithms for Multimodal Optimization. International Symposium on Stochastic Algorithms*; Springer: Berlin/Heidelberg, Germany, 2009; pp. 169–178.
13. Li, X. A New Intelligent Optimization-Artificial Fish Swarm Algorithm. Doctor Thesis, Zhejiang University, Zhejiang, China, 2003.
14. Pan, W.-T. A new fruit fly optimization algorithm: Taking the financial distress model as an example. *Knowl.-Based Syst.* **2012**, *26*, 69–74. [CrossRef]
15. Mirjalili, S. Dragonfly algorithm: A new meta-heuristic optimization technique for solving single-objective, discrete, and multi-objective problems. *Neural Comput. Appl.* **2016**, *27*, 1053–1073. [CrossRef]

16. Xu, L.; Jia, H.; Lang, C.; Peng, X.; Sun, K. A novel method for multilevel color image segmentation based on dragonfly algorithm and differential evolution. *IEEE Access* **2019**, *7*, 19502–19538. [CrossRef]
17. Tharwat, A.; Gabel, T.; Hassanien, A.E. Parameter optimization of support vector machine using dragonfly algorithm. In *International Conference on Advanced Intelligent Systems and Informatics*; Springer: Berlin/Heidelberg, Germany, 2017; pp. 309–319.
18. Zhang, Z.; Hong, W.-C. Electric load forecasting by complete ensemble empirical mode decomposition adaptive noise and support vector regression with quantum-based dragonfly algorithm. *Nonlinear Dyn.* **2019**, *98*, 1107–1136. [CrossRef]
19. Amroune, M.; Bouktir, T.; Musirin, I. Power system voltage stability assessment using a hybrid approach combining dragonfly optimization algorithm and support vector regression. *Arab. J. Sci. Eng.* **2018**, *43*, 3023–3036. [CrossRef]
20. Sureshkumar, K.; Ponnusamy, V. Power flow management in micro grid through renewable energy sources using a hybrid modified dragonfly algorithm with bat search algorithm. *Energy* **2019**, *181*, 1166–1178. [CrossRef]
21. Suresh, V.; Sreejith, S. Generation dispatch of combined solar thermal systems using dragonfly algorithm. *Computing* **2017**, *99*, 59–80. [CrossRef]
22. Babayigit, B. Synthesis of concentric circular antenna arrays using dragonfly algorithm. *Int. J. Electron.* **2018**, *105*, 784–793. [CrossRef]
23. Hammouri, A.I.; Samra, E.T.A.; Al-Betar, M.A.; Khalil, R.M.; Alasmer, Z.; Kanan, M. A dragonfly algorithm for solving traveling salesman problem. In Proceedings of the 2018 8th IEEE International Conference on Control System, Computing and Engineering (ICCSCE), Penang, Malaysia, 23–25 November 2018; pp. 136–141.
24. Mafarja, M.M.; Eleyan, D.; Jaber, I.; Hammouri, A.; Mirjalili, S. Binary dragonfly algorithm for feature selection. In Proceedings of the 2017 International Conference on New Trends in Computing Sciences (ICTCS), Amman, Jordan, 11–13 October 2017; pp. 12–17.
25. Kennedy, J.; Eberhart, R.C. A discrete binary version of the particle swarm algorithm. In Proceedings of the 1997 IEEE International Conference on Systems, Man, and Cybernetics. Computational Cybernetics and Simulation, Orlando, FL, USA, 12–15 October 1997; pp. 4104–4108.
26. Mirjalili, S.; Mirjalili, S.M.; Yang, X.-S. Binary bat algorithm. *Neural Comput. Appl.* **2014**, *25*, 663–681. [CrossRef]
27. Hammouri, A.I.; Mafarja, M.; Al-Betar, M.A.; Awadallah, M.A.; Abu-Doush, I. An improved dragonfly algorithm for feature selection. *Knowl. Based Syst.* **2020**, *203*, 106131. [CrossRef]
28. Proakis, J.G.; Salehi, M.; Zhou, N.; Li, X. *Communication Systems Engineering*; Prentice Hall New Jersey: Hoboken, NJ, USA, 1994; Volume 2.
29. Pampara, G.; Franken, N.; Engelbrecht, A. Combining particle swarm optimization with angle modulation to solve binary problems. *IEEE Congr. Evol. Comput.* **2005**, *1*, 89–96.
30. Pampara, G.; Engelbrecht, A.; Franken, N. Binary differential evolution. In Proceedings of the IEEE Congress on Evolutionary Computation Vancouver, BC, Canada, 16–21 July 2006; pp. 1873–1879.
31. Dong, J.; Wang, Z.; Mo, J. A Phase Angle-Modulated Bat Algorithm with Application to Antenna Topology Optimization. *Appl. Sci.* **2021**, *11*, 2243. [CrossRef]
32. Reynolds, C.W. Flocks, Herds, and Schools: A Distributed Behavioral Model. *ACM SIGGRAPH Comput Gr.* **1987**, *21*, 25–34. [CrossRef]
33. Too, J.; Abdullah, A.R.; Mohd Saad, N.; Mohd Ali, N.; Tee, W. A New Competitive Binary Grey Wolf Optimizer to Solve the Feature Selection Problem in EMG Signals Classification. *Computers* **2018**, *7*, 58. [CrossRef]
34. Jain, M.; Singh, V.; Rani, A. A novel nature-inspired algorithm for optimization: Squirrel search algorithm. *Swarm Evol. Comput.* **2019**, *44*, 148–175. [CrossRef]
35. Tsai, H.C.; Tyan, Y.Y.; Wu, Y.W.; Lin, Y.H. Isolated particle swarm optimization with particle migration and global best adoption. *Eng. Optim.* **2012**, *44*, 1405–1424. [CrossRef]
36. Kashan, M.H.; Kashan, A.H.; Nahavandi, N. A novel differential evolution algorithm for binary optimization. *Comput. Optim. Appl.* **2013**, *55*, 481–513.
37. Yılmaz, S.; Küçüksille, E.U. A new modification approach on bat algorithm for solving optimization problems. *Appl. Soft Comput.* **2015**, *28*, 259–275. [CrossRef]
38. Hu, T.; Kahng, A.B. *Linear and Integer Programming Made Easy*; Springer: Berlin/Heidelberg, Germany, 2016.
39. Mavrotas, G.; Diakoulaki, D.; Kourentzis, A. Selection among ranked projects under segmentation, policy and logical constraints. *Eur. J. Oper. Res.* **2008**, *187*, 177–192. [CrossRef]
40. Zhang, Y.; Song, X.-F.; Gong, D.-W. A return-cost-based binary firefly algorithm for feature selection. *Inf. Sci.* **2017**, *418*, 561–574. [CrossRef]
41. Zhang, L.; Shan, L.; Wang, J. Optimal feature selection using distance-based discrete firefly algorithm with mutual information criterion. *Neural Comput. Appl.* **2017**, *28*, 2795–2808. [CrossRef]
42. Mafarja, M.M.; Mirjalili, S. Hybrid binary ant lion optimizer with rough set and approximate entropy reducts for feature selection. *Soft Comput.* **2019**, *23*, 6249–6265. [CrossRef]
43. Kulkarni, A.J.; Shabir, H. Solving 0–1 knapsack problem using cohort intelligence algorithm. *Int. J. Mach. Learn. Cybern.* **2016**, *7*, 427–441. [CrossRef]
44. Wu, H.; Zhang, F.-M.; Zhan, R.; Wang, S.; Zhang, C. A binary wolf pack algorithm for solving 0-1 knapsack problem. *Syst. Eng. Electron.* **2014**, *36*, 1660–1667.
45. Zou, D.; Gao, L.; Li, S.; Wu, J. Solving 0–1 knapsack problem by a novel global harmony search algorithm. *Appl. Soft Comput.* **2011**, *11*, 1556–1564. [CrossRef]